

Real-time Progressive 3D Semantic Segmentation for Indoor Scenes

Quang-Hieu Pham¹ Binh-Son Hua² Duc Thanh Nguyen³ Sai-Kit Yeung¹

¹Singapore University of Technology and Design

²Tokyo University

³Deakin University

Abstract. The widespread adoption of autonomous systems such as drones and assistant robots has created a need for real-time high-quality semantic scene segmentation. In this paper, we propose an efficient yet robust technique for on-the-fly dense reconstruction and semantic segmentation of 3D indoor scenes. To guarantee real-time performance, our method is built atop small clusters of voxels and a conditional random field with higher-order constraints from structural and object cues, enabling progressive dense semantic segmentation without any precomputation. We extensively evaluate our method on different indoor scenes including kitchens, offices, and bedrooms in the SceneNN and ScanNet datasets and show that our technique consistently produces state-of-the-art segmentation results in both qualitative and quantitative experiments.

1 Introduction

Recent hardware advances in consumer-grade depth cameras have made high-quality reconstruction of indoor scenes feasible. RGB-D images have been used to boost the robustness of numerous scene understanding tasks in computer vision, such as object recognition, object detection, and semantic segmentation. While scene understanding using color or RGB-D images is a well explored topic [1,2,3], good solutions for the same task in the 3D domain have been demanding, particularly, those can produce accurate and high-quality semantic segmentation. Directly applying techniques for color and RGB-D images to the 3D domain is a straightforward idea and would not yield competent accuracy.

In this work, we propose a new real-time technique for high-quality dense semantic segmentation of 3D scene. The backbone of our work is a novel conditional random field (CRF) designed to infer an optimal set of labels from the predictions of a neural network. In contrast to traditional models, our CRF accepts additional constraints from unsupervised object analysis, resulting in high-quality segmentation while preserving real-time performance. An example output from our proposed method is shown in Figure 1. Experiments proved that our algorithm is capable of producing high-quality semantic segmentation. In summary, our contributions are:

- A higher-order conditional random field that can resolve noisy predictions from a deep neural network into a coherent 3D dense segmentation, using object-level information.

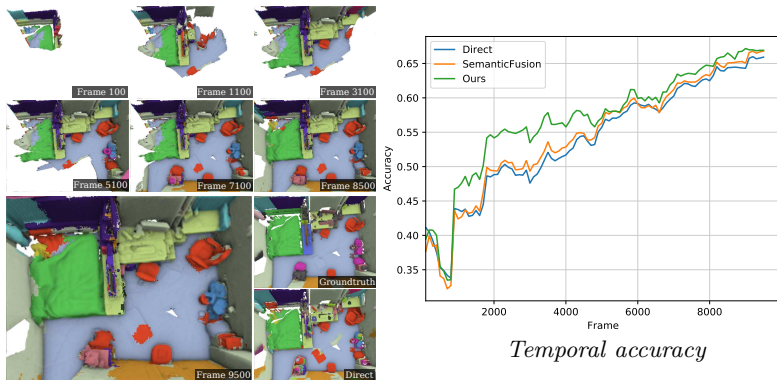


Fig. 1: Progressive semantic segmentation of a 3D scene in real-time. Our method can resolve error in segmentation while scanning. Notice the error segment on the bed gradually getting fixed as the user scanning through the scene.

- A real-time dense reconstruction pipeline with an efficient voxel clustering technique to enable real-time full scene inference while scanning.
- A thorough evaluation of state-of-the-art real-time semantic segmentation algorithms on two indoor datasets, namely SceneNN [4] and ScanNet [5]. Beyond category-based semantic segmentation, we also extend our method to instance-based semantic segmentation and provide the first baseline evaluation of real-time instance segmentation on the SceneNN dataset.

2 Related Work

Conditional random field. The CRF model, often containing a unary and pairwise terms, is commonly used in the segmentation problem. There are numerous improvements over the original model that were proposed. One of such examples is Krähenbühl and Koltun [6] with their efficient message passing method to perform inference on a fully-connected CRF model.

Recently, immense advances in deep learning have replaced hand-crafted descriptors with high-level automatic features from CNN for many scene understanding tasks like object classification, detection, and segmentation. To boost segmentation results from CNN, CRF can be used as a post-processing step [7]. Follow-up works [8,9] showed that CRF can be embedded as layers within a deep neural network and its parameters can be learnt via backpropagation.

While representing CRF by a recurrent neural network [8,9] is advantageous, applying such end-to-end framework to our problem poses some challenges. First in the context of progressive 3D reconstruction and segmentation, 2D predictions from multiple views have to be combined to produce the labeling of 3D model, which is not supported in the previous method where only the segmentation of one single image is predicted. Second, their methods is computationally demanding which does not fit our real-time requirement. Third, the number of 2D images used to calculate the unaries is not fixed, compared to using only one input image as in previous approaches. In this work, we instead run the CRF separately on 3D after processing 2D semantic predictions from a convolutional neural network.

Indoor scene semantic segmentation. We discuss recent advances in semantic segmentation for indoor scenes. Silberman *et al.* [1] proposed a technique to segment cluttered indoor scenes into floor, walls, objects and reconstruct support relationships. Their well-known NYUv2 dataset has since sparked new research interests in semantic segmentation using RGBD images.

Long *et al.* [3] adapted neural networks originally trained for classification to solve semantic segmentation by appending a fully connected layer to the existing architecture. While achieving state-of-the-art results, this method tends to produce inaccuracies along object boundaries. To address this issue, different techniques [10,11] has been proposed to improve the segmentation results. Some recent works also explored instance segmentation [12,13], but such techniques only work with individual color or RGB-D images.

In the 3D domain, Song *et al.* [14] proposed a network architecture for semantic scene completion on 3D volume. Point-based deep learning [15,16,17] took another direction and attempted to learn the segmentation directly from unordered point clouds. While the results from these neural networks are impressive, they are more suitable for offline usage.

Real-time dense reconstruction. With the introduction of consumer-grade RGBD sensors such as the Microsoft Kinect, and the ever-increasing GPUs computation power to process these data, an online dense reconstruction system is entirely feasible. The seminal KinectFusion paper [18] showed us how to construct such system. To overcome the spatial constraints in the original KinectFusion implementation, which prohibits large-scale 3D scanning, Nießner *et al.* [19] used voxel hashing to reduce the memory footprint.

Valentin *et al.* [20] proposed an interactive scanning system where the segmentation is learnt from user inputs. Unlike them, our method is completely automatic without the need of user interaction, and thus more suitable for robotics applications. To our knowledge, the closest work to ours in this aspect is by McCormac *et al.* [21]. Their method obtains segmentation in 2D by using a deep neural network that takes color and depth images as input. The 2D labels are then propagated to the scene. Noise and label inconsistencies are resolved by a smoothing process using a conditional random field.

Directly fusing 2D predictions into 3D model has one major drawback, that is it only considers each vertex in the scene individually, imposing both spatial and temporal inconsistencies. Our argument is that to obtain a coherent, high-quality segmentation, vertices in the same object should be consider as a whole in the model. Moreover, noises and inconsistencies should be fixed regularly as the user scanning through the scene. We formulate this idea by using a higher-order CRF model with additional object cues, combining with an efficient dense reconstruction scheme. As shown in Figure 1, our method is able to recover from poor initial segmentation and can help resolving label inconsistencies, while maintaining real-time performance.

3 Real-time RGB-D Reconstruction

We now introduce our proposed method for the progressive dense semantic segmentation problem. An overview of our framework is shown in Figure 2.

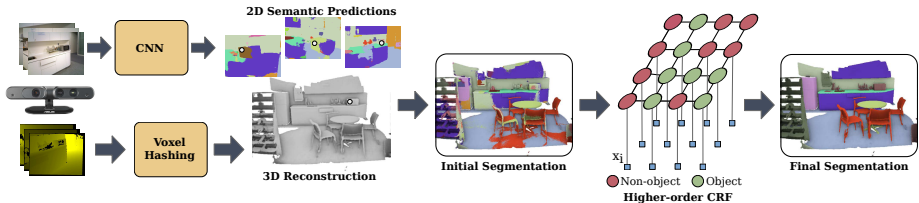


Fig. 2: Overview of our progressive indoor scene segmentation method. From continuous frames of an RGB-D sensor, our system performs on-the-fly reconstruction and semantic segmentation. All of our processing is performed on a frame-by-frame basis in an online fashion, thus useful for real-time applications.

3.1 Semantic label fusion

Our online scanning system is built on the Voxel Hashing [19] pipeline, recovering both geometric and semantic information of the scene in real time. In principal, given the incoming prediction from CNN, we must update the semantic label for each active voxel accordingly, using the same integration process as described in KinectFusion [18]. For this problem, McCormac *et al.* [21] store a full discrete probability distribution in each voxel, and update it by using recursive Bayesian rule. However, doing so requires a large amount of memory and does not scale well with the number of semantic classes. We employ the update process proposed by Cavallari and Di Stefano [22], where each voxel only stores the current best label and its confidence.

3.2 Progressive supervoxel clustering

Now we explain in details our supervoxel clustering method, which will provide a new domain to define our CRF with higher-order constraints. Our supervoxel clustering method resembles previous local k-means clustering techniques such as VCCS [23] or SLIC [24]. The main difference in our supervoxel clustering method is that, to amortize the computation cost, we create supervoxels in a progressive manner, performing one clustering iteration at a time, which will adapt better to the changes in the current reconstructed scene. Since normal computation on every voxels is quite costly, we use only voxel color and position in our distance measure D :

$$D = \sqrt{\frac{\alpha D_c}{n_c} + \frac{\beta D_s}{n_s}} \quad (1)$$

where D_c and D_s are the color and spatial distances, with n_c and n_s act as the normalizers; α and β control the relative weighting of color and spatial distances. In all of our experiments, we set α and β to 1; the normalization values n_c and n_s are based on the chosen voxel size which is $0.008m$ and color space (CIELab).

Suppose that an existing set of supervoxels are already provided. For an incoming RGB-D frame at time t , after camera pose estimation, we can find out the current active set V_t of voxels using an inside/outside check on the current

camera frustum. Our goal is to assign each of these voxels into a supervoxel (or cluster). This process is as follows: first new seeds are sampled on uninitialized regions, based on a chosen spatial interval S . For each active voxel, we assign it to the nearest cluster according to the distance in Equation 1. Next, we update the centers information based on the new cluster assignment. This process is repeated for every incoming RGB-D frame, providing a “live” unsupervised over-segmentation of the scene.

Our progressive supervoxel building scheme fits well into the common dense RGB-D reconstruction pipelines such as KinectFusion [18] or Voxel Hashing [19], and can be implemented effectively on the GPU. In practice, we only consider voxels close to the surface, based on their distance-to-surface values. Performing inference on these supervoxels significantly reduces the domain size of our CRF, and thus paves the way for real-time semantic segmentation.

3.3 Real-time object proposal

For 3D object proposal, Karpathy *et al.* [25] presented a method for discovering object models from 3D meshes of indoor environments. Their method works first generates object candidates by over-segmenting the scene on different thresholds. The candidates are then evaluated and suppressed based on geometric metrics to produce the final proposals. Kanazaki [26] proposed an extension of selective search for object proposal for 3D point cloud.

One common drawback of these methods is their high computation cost, since they require a costly object analysis on different scales. This process has to be done for every update, which hinders real-time performance. In this work, we explore on a new direction for object proposal, in which we propose object based on statistical evidences.

Our object proposal is come from a simple observation: given an object and multiple observations, it should be identified as an object in most of the corresponding 2D semantic predictions. Hence, for each incoming RGB-D frame, we update the objectness score of a vertex given its current predicted label. Specifically, we decrease the objectness score if the prediction is a non-object label, *i.e.* wall, floor, or ceiling; and increase it otherwise. To perform object proposal, we employ an efficient graph-based segmentation algorithm from Felzenszwalb and Huttenlocher [27]. The edge weight between two supervoxels is defined as $w_{i,j} = w_{i,j}^\alpha + w_{i,j}^\eta + w_{i,j}^\omega$ where $w_{i,j}^\alpha$ and $w_{i,j}^\eta$ is the color and normal weights, respectively; $w_{i,j}^\omega$ is the absolute difference in objectness. We normalize the each of the weights accordingly.

4 Higher-order CRF Refinement

Using CRF as a post-processing step is a common technique in semantic segmentation. However, for real-time applications, there are two limitations that we must address. First is the classification errors caused by inconsistencies, called ‘bleeding’, that is also reported by Valentin *et al.* [28]. The second issue is scalability, since the number of vertices often grow significantly to millions when

new parts of the scene are discovered, causing CRF optimizations to become much slower over time. In this work, we address both limitations by introducing a CRF model with *higher-order constraints* on *supervoxels* to perform online segmentation. This model is lightweight and very easy to compute, allowing it to work on a wide range of indoor scenes, while remaining computationally efficient for real-time use.

Now we explain our higher-order CRF model for label refinement in details. Let \mathcal{M}^t be the 3D geometry at time t with N^t supervoxels. In a semantic segmentation problem, we attempt to assign every supervoxel with a label from a discrete label space, denoted $\mathcal{L} = \{l_1, l_2, \dots, l_L\}$. Let $\mathbf{X}^t = \{x_1^t, \dots, x_N^t\}$ define a set of random variables, one for each supervoxel, where $x_i^t \in \mathcal{L}$. An assignment of every x_i^t will be a solution to the segmentation problem. For shorter notation, we will drop all the time annotation from now on.

Given the above definitions, we define a graph \mathcal{G} where each vertex is from \mathbf{X} . In addition, let \mathcal{C} be the set of cliques in \mathcal{G} , given by an object proposal method. For every clique $r \in \mathcal{C}$, we can select a corresponding set of random variables \mathbf{x}_r that belongs to r . Our CRF model introduces three new types of higher-order potential, namely objectness potential ψ^O , consistency potential ψ^C and object relationship potential ψ^R . These terms are later explained in Sections 4.1, 4.2, and 4.3, respectively. Our complete CRF model is then defined as follows

$$E(\mathbf{X}) = \sum_i \varphi(x_i) + \sum_{i < j} \psi^P(x_i, x_j) + \sum_{r \in \mathcal{C}} \psi^O(\mathbf{x}_r) + \sum_{r \in \mathcal{C}} \psi^C(\mathbf{x}_r) + \sum_{r, q \in \mathcal{E}(\mathcal{C})} \psi^R(\mathbf{x}_r, \mathbf{x}_q) \quad (2)$$

where $\varphi(x_i)$ and $\psi^P(x_i, x_j)$ are the unary and pairwise terms used in the conventional dense CRF model. The unary term represent the prediction from a local classifier. In our case, it is obtained from fusing CNN predictions during reconstruction.

The pairwise (smoothness) potential $\psi^P(x_i, x_j)$ is parameterized by a Gaussian kernel

$$\psi^P(x_i, x_j) = \mu_{ij} \exp\left(-\frac{|p_i - p_j|}{2\theta_\alpha^2} - \frac{|n_i - n_j|}{2\theta_\beta^2}\right) \quad (3)$$

where μ_{ij} is the label compatibility function between x_i and x_j given by the Potts model; p_i and n_i are the location and normal of the i^{th} supervoxel; θ_α and θ_β are standard deviations of the kernel.

4.1 Objectness potential

The term $\psi^O(\mathbf{x}_r)$ captures the mutual agreement between the objectness score of a clique and its semantic label. Ideally, we would want a clique with low objectness score to take a non-object label, *i.e.* wall, floor, or ceiling; and inversely. To model the objectness potential of a clique, we first introduce latent binary random

variables $y_1, \dots, y_{|\mathcal{C}|}$. y_k can be interpreted as follows: if the k^{th} proposal has been found to be an object, then y_k is 1, otherwise it will be 0. Let \mathcal{O} be the subset of \mathcal{L} , which comprises of object classes in the label space. We can then define our objectness potential

$$\psi^O(\mathbf{x}_r) = \begin{cases} \frac{1}{|\mathbf{x}_r|} \sum_{i \in \mathbf{x}_r} [x_i \notin \mathcal{O}], & \text{if } y_r = 1, \\ \frac{1}{|\mathbf{x}_r|} \sum_{i \in \mathbf{x}_r} [x_i \in \mathcal{O}], & \text{if } y_r = 0, \end{cases} \quad (4)$$

where $[\cdot]$ is a function that converts a logical proposition into 1 if the condition is satisfied, otherwise it would be 0. The purpose of this term is to correct misclassification error in the local classifier, based on external unsupervised information from object proposal.

4.2 Label consistency

The term $\psi^C(\mathbf{x}_r)$ enforces regional consistency in semantic segmentation. Since we want vertex labels in the same clique to be homogeneous, the cost function penalizes label based on its frequency in the clique. Let $f_r(l_k)$ be the normalized frequency of label $l_k \in \mathcal{L}$ inside the r^{th} clique, which is of the range between 0 and 1. The consistency cost will be the entropy of the underlying distribution:

$$\psi^C(\mathbf{x}_r) = - \sum_{l_k \in \mathcal{L}} f_r(l_k) \log f_r(l_k) \quad (5)$$

This term dampens infrequent labels in a clique. In experiments, we observed that the consistency term helps in getting rid of low-frequency errors in the output segmentation. We observed that the label consistency cost helps in fixing segmentation ‘bleeding’, as shown in Figure 5.

4.3 Region relationship

The relationship potential ψ^R encodes the relation between two regions (cliques) and their semantic labels. This cost is applied on neighboring regions, based on voxel connectivity. In our model, the term $\psi^R(\mathbf{x}_r, \mathbf{x}_q)$ is defined based on the co-occurrence of class labels in the regions. Specifically, let $\mathcal{E}(\mathcal{C}) \subset \mathcal{C} \times \mathcal{C}$ be the edges between connected cliques. The object relationship cost between \mathbf{x}_r and \mathbf{x}_q is defined as follows,

$$\psi^R(\mathbf{x}_r, \mathbf{x}_q) = - \sum_{l_i \in \mathcal{L}} \sum_{l_j \in \mathcal{L}} \log (f_r(l_i) f_q(l_j) A_{l_i, l_j}) \quad (6)$$

where A_{l_i, l_j} is the co-occurrence cost based on the class labels l_i and l_j and designed such that the more often l_i and l_j co-occur, the greater A_{l_i, l_j} is. This cost acts like a prior to prevent uncommon label transition, *e.g.* chair to ceiling, ceiling to floor, etc; and can be learnt beforehand. f_r and f_q are the label frequencies, as presented in (5).

In our CRF model, each term is accompanied with a weight to balance their values that we omit them in our formulas for better clarity. We learn these weights by grid search, and keep them unchanged in every experiment. Finally, semantic segmentation can be done by minimizing the energy function $E(\mathbf{X})$ defined in (2). In this paper, we adopt the variational mean field method [6] for efficiently optimizing $E(\mathbf{X})$. Details of the inference process can be found in the supplementary material.

4.4 Instance segmentation

Beyond category-based semantic segmentation, our proposed technique can be easily extended to output instance-based semantic segmentation in real-time, which we refer as *instance segmentation* for brevity. In general, the CRF is changed to output an additional label that indicates instance ID. Other terms and the optimization are kept unchanged.

For each vertex to label with the CRF, it is now required to initialize the unary term with probabilities about instance IDs. The naive approach could be to utilize a deep neural network that can predict instance labels in 2D, and then propagate the labels from 2D to 3D as in the category-based semantic segmentation case. However, this approach requires to track instance IDs over time since most networks can only process one frame at a time, which is in fact a challenging problem.

Therefore, we instead opt for a more flexible design as follows. We still utilize the same category-based semantic segmentation network in 2D as before, and initialize instances directly in 3D using a connected component algorithm. This approach allows our system to perform both category-based and instance-based semantic segmentation by just utilizing a single deep neural network that outputs category-based semantic segmentation.

Our 3D instance segmentation algorithm is as follows. We first create 4 special instances for unknown, wall, floor, and ceiling regions in the scene, respectively. At each frame, we perform reprojection to the current camera frustum to determine the number of current instances, namely K . Our higher-order CRF will optimize the instance labels of supervoxels that lie in the camera frustum, where the labels are in the label space $\mathcal{L} = \{l_1, l_2, \dots, l_{K+4}\}$. To create cliques, we use a connected component algorithm to connect supervoxels in a neighborhood with the same category. The instance segmentation results are then fused back into the current 3D model, where each voxel now holds an instance probability instead of category probability. At every frame, we take the largest clique that belongs to the unknown instance and spawn a new instance at its location.

5 Experiments

Implementation details. To get the 2D segmentation predictions, we use SegNet [11] trained on SUN RGB-D dataset. The CRF inference code is based on the publicly available implementation from Krähenbühl and Koltun [6]. For real time usage, we only run the CRF inference for one iteration at a time. Full video of our online implementation can be found in the supplementary materials.

ID	Direct	SF	Ours		ID	Direct	SF	Ours	
	Class	Class	Class	Instance		Class	Class	Class	Instance
011	0.770	0.776	0.800	0.521	205	0.635	0.642	0.629	0.508
016	0.607	0.625	0.680	0.342	206	0.766	0.778	0.775	0.417
030	0.584	0.597	0.658	0.568	207	0.559	0.568	0.596	0.172
061	0.751	0.777	0.809	0.591	213	0.539	0.551	0.561	0.478
078	0.497	0.515	0.535	0.349	223	0.669	0.689	0.729	0.409
086	0.622	0.646	0.668	0.350	231	0.655	0.656	0.660	0.692
089	0.558	0.573	0.618	0.236	243	0.538	0.553	0.595	0.144
096	0.659	0.668	0.666	0.265	255	0.423	0.439	0.558	0.486
098	0.601	0.600	0.623	0.321	272	0.602	0.614	0.612	0.203

Table 1: Comparison of category-based semantic segmentation accuracy on typical scenes in SceneNN dataset. We report performances on office, kitchen, bedroom, and other scenes. Our proposed CRF model consistently outperforms the naive approach that directly fuses neural network predictions to 3D (Direct) [22], and SemanticFusion (SF) [21]. Please also refer to the supplementary document for weighted IoU scores. The fifth column further reports the accuracy of the instance-based semantic segmentation task.

Experiment setup. In SemanticFusion [21], the authors chose to evaluate on NYUv2 dataset, a popular 2D dataset for semantic segmentation task. However, evaluation in 2D by projecting labels from 3D model to 2D image is not completely sound; since 2D images cannot cover the entire scene, and there are potential ambiguities when doing 2D-3D projection. To tackle this problem, we perform our evaluation on SceneNN [4] and ScanNet [5], which are two 3D mesh datasets with dense annotations. Our evaluation can later act as a reference benchmark for real-time 3D scene segmentation.

We adopt two common metrics from 2D semantic segmentation for our 3D evaluation, namely vertex accuracy (A) and frequency weighted intersection over union ($wIoU$). We only showed results with accuracy metric in this section. Please see our supplementary document for evaluations with $wIoU$.

Online semantic segmentation We compare our approach to the following methods: (1) Direct label fusion [22]; (2) SemanticFusion [21]. For fair comparison, all of our online results are reconstructed with the same camera trajectories, using the same semantic predictions from SegNet.

We present the performance comparison of our algorithm in various indoor settings. The results for each scene in our evaluation are shown in Table 1. Our method outperforms SemanticFusion and the direct fusion approach in almost all of the scenes. Qualitative results also show that our method is less subjected to noises and inconsistencies in segmentation compared to other approaches, especially on object boundaries.

Offline semantic segmentation. We further investigate our model robustness subject to different types of initial segmentation. We perform the experiment in

Acc.	SegNet		FCN-8s		SSCNet		Acc.	SegNet		FCN-8s		SSCNet		
	ID	Base	Ours	Base	Ours	Base		Ours	ID	Base	Ours	Base	Ours	Base
	011	0.747	0.837	0.667	0.743	0.475	0.497	205	0.610	0.678	0.562	0.661	0.332	0.680
	016	0.556	0.714	0.580	0.623	0.648	0.798	206	0.659	0.812	0.626	0.828	0.861	0.834
	030	0.554	0.668	0.584	0.704	0.505	0.510	207	0.673	0.734	0.556	0.589	0.596	0.634
	061	0.549	0.841	0.324	0.457	0.700	0.693	213	0.597	0.683	0.579	0.671	0.543	0.552
	078	0.542	0.666	0.551	0.663	0.515	0.588	223	0.648	0.758	0.693	0.760	0.644	0.639
	086	0.587	0.686	0.491	0.631	0.543	0.517	231	0.624	0.697	0.621	0.741	0.531	0.621
	089	0.581	0.651	0.605	0.667	0.491	0.631	243	0.655	0.667	0.663	0.663	0.591	0.734
	096	0.615	0.683	0.577	0.619	0.631	0.658	255	0.521	0.654	0.577	0.718	0.547	0.661
	098	0.653	0.656	0.709	0.740	0.314	0.706	272	0.607	0.703	0.586	0.706	0.698	0.777

Table 2: Accuracy scores of the offline semantic segmentation on SceneNN [4]. Our proposed CRF model consistently improves the accuracy of initial predictions from SegNet, FCN-8s [3] and SSCNet [14]. Please refer to the supplementary document for weighted IoU scores and the results on ScanNet [5].

offline setting, taking unary predictions from different neural networks and refine them using our proposed higher-order CRF. For the offline experiment, since the meshes are already provided, we run CRF inference directly on a per-vertex level to produce highest segmentation quality. All of the neural networks are trained on the NYUv2 dataset [1].

Results from SegNet [11], SSCNet [14], and FCN-8s [3] are shown in Table 2. Note that SSCNet produces a $60 \times 36 \times 60$ volume low-resolution segmentation for entire scene due to memory constraints, so we need to resample to a higher resolution. In contrast, our 2D-to-3D approach can achieve segmentation on high-resolution meshes in real-time. Again, our method improves SegNet by 10% in accuracy, SSCNet by 8%, and FCN by 9%. This shows that our proposed CRF performs robustly to different kinds of unary. See Figure 5 for more detailed qualitative comparisons.

Per-class accuracy. We measured per-class accuracy of our method and SemanticFusion [21] (see Table 3 below). The results show that our method consistently outperforms SemanticFusion. On average, we increase accuracy by 6% compared to SemanticFusion and 11% compared to the direct fusion method.

Temporal accuracy Since our method can be run in real-time, we evaluate the segmentation accuracy over time. For every scene, we measure the accuracy every 100 frames. The progressive results are shown in Figure 6.

We observe that the accuracy over time is not stable due to temporal inconsistencies from the CNN predictions. Results also suggest that our method *consistently* outperforms other methods in a long run, not just only at a certain time period. This kind of unstable performance while scanning is interesting, and a method that can optimize the performance over time would be valuable.

Ablation study To further understand the performance of our CRF model, we carry out an ablation study to see the effect of each CRF term on the result

	wall	floor	cabinet	bed	chair	sofa	table	door
Direct	0.710	0.914	0.471	0.309	0.430	0.555	0.557	0.313
SF	0.728	0.944	0.570	0.343	0.463	0.578	0.701	0.386
Ours	0.750	0.965	0.620	0.375	0.649	0.661	0.698	0.513
	window	bookshelf	picture	counter	blinds	desk	curtain	pillow
Direct	0.252	0.839	0.202	0.266	0.215	0.236	0.643	0.268
SF	0.315	0.940	0.225	0.371	0.210	0.281	0.830	0.294
Ours	0.425	0.947	0.121	0.551	0.231	0.408	1.000	0.253
	clothes	ceiling	books	fridge	television	paper	nightstand	sink
Direct	0.197	0.705	0.426	0.700	0.212	0.119	0.076	0.380
SF	0.236	0.800	0.524	0.803	0.277	0.320	0.090	0.388
Ours	0.290	0.858	0.603	0.823	0.643	0.097	0.145	0.342
	lamp	shelves	bag	structure	furniture	prop	Average	
Direct	0.284	0.000	0.226	0.121	0.110	0.275	0.367	
SF	0.391	0.000	0.214	0.169	0.016	0.291	0.423	
Ours	0.583	0.000	0.364	0.262	0.018	0.312	0.484	

Table 3: Per-class accuracy of 40 NYUDv2 classes on SceneNN dataset from direct fusion with predictions from SegNet, SemanticFusion (SF) and ours. Note that some of the classes are missing from the evaluation data. Best view in color.

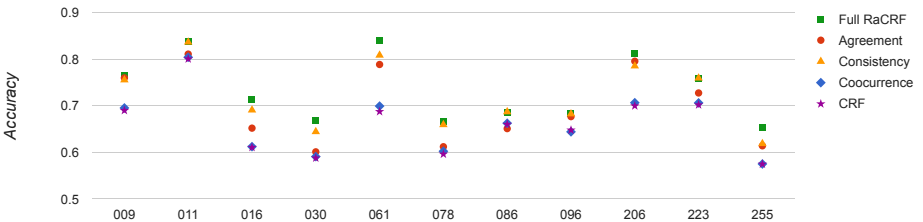


Fig. 3: Ablation study on the effects of different CRF terms. There is usually a noticeable gap between the performances of the conventional dense CRF and ours. In addition, individual term helps improving the segmentation accuracy. This study also shows the importance of consistency in semantic segmentation.

segmentation. We execute three runs on 10 scenes, each run enables only one term in our CRF model, and record their performances. Figure 3 visualizes the results on these 10 scenes. In general, running full higher-order model achieves the best performance; moreover, individual term is able to surpass the base dense CRF model consistently. Consistency contributes the most in the performance boost, which validates our initial hypothesis that object-level information is crucial when performing dense semantic segmentation.

Instance segmentation We evaluate instance segmentation numerically using average precision [29] with overlap value of 50%. The results are shown in Table 1. Figure 4 visualizes the instance segmentation of some typical indoor scenes using our approach. In general, such results could serve as a baseline to compare with more sophisticated real-time 3D instance segmentation technique in the future.

Runtime benchmarking Runtime benchmarking are performed on a desktop with an Intel Core i7-5820K 3.30GHz CPU, 32GB RAM, and an NVIDIA Titan X

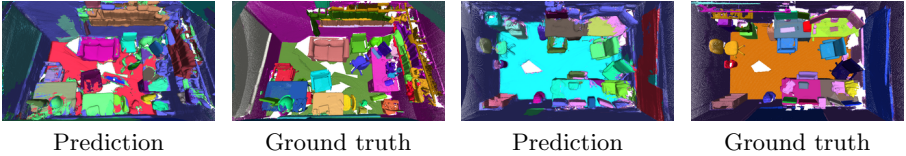
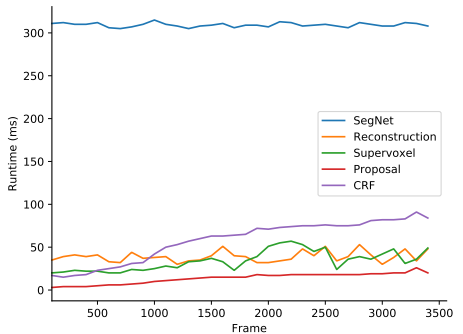


Fig. 4: Instance-based semantic segmentation on scenes in the SceneNN dataset [4].

GPU. The average runtime breakdown of each step in the pipeline is demonstrated in the inline figure (below). Specifically, it takes 309.3ms on average to run a single forward pass of neural network. Building supervoxels takes 34.1ms. CRF with higher-order constraints requires additional 57.9 ms. As can be seen, over time when more regions in the scene are reconstructed, our semantic segmentation still takes constant running time on average.

Specifically, it takes 309.3ms on average to run a single forward pass of neural network. Building supervoxels takes 34.1ms. CRF with higher-order constraints requires additional 57.9 ms. As can be seen, over time when more regions in the scene are reconstructed, our semantic segmentation still takes constant running time on average. For online operation, we only run the CNN prediction once every 10 frames to maintain a high frame rate. Compared to running CNN prediction every frame (Table 2), real time results (Table 1) drop about 5% accuracy on average, but the speed gain is more than 8 times. In general, our online system performs all the necessary computations at a rate of 10-15 FPS.



Specifically, it takes 309.3ms on average to run a single forward pass of neural network. Building supervoxels takes 34.1ms. CRF with higher-order constraints requires additional 57.9 ms. As can be seen, over time when more regions in the scene are reconstructed, our semantic segmentation still takes constant running time on average. For online operation, we only run the CNN prediction once every 10 frames to maintain a high frame rate. Compared to running CNN prediction every frame (Table 2), real time results (Table 1) drop about 5% accuracy on average, but the speed gain is more than 8 times. In general, our online system performs all the necessary computations at a rate of 10-15 FPS.

Limitations There are two possible sources of inaccuracy in our technique. First, our model encourages consistency, which sometimes may produce over-regularized segmentation. Second, inaccurate object analysis might reduce the final accuracy of the CRF. For example, when there is a thin object on top of a planar region, the region proposal algorithm might group them into a single region. Please see our supplemental document for a detailed analysis of this case.

6 Conclusion

Our system demonstrates the capability to integrate semantic segmentation into real-time indoor scanning by optimizing the predictions from a 2D neural network with a novel region-aware CRF model. The results and ground truth category-based and instance-based semantic segmentation will be made publicly available.

Designing deep neural networks and conditional random field for semantic segmentation is still an on-going research direction. Our approach is designed to be general so that it can still incorporate new deep learning techniques emerged

in the near future. The results from our system can further be used in other interactive or real-time applications, e.g., for furniture arrangement [30], object manipulation and picking in robotics, or augmented reality applications.

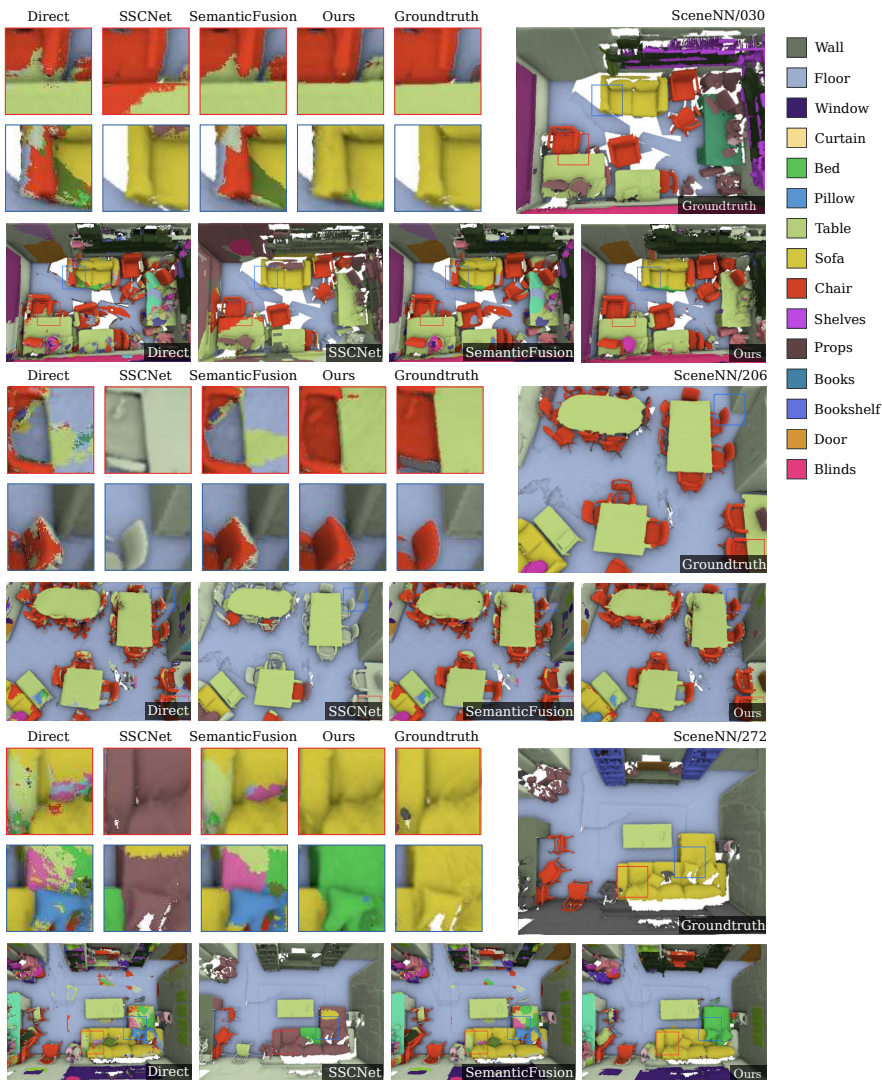


Fig. 5: Some qualitative results on SceneNN. The results are shown on small, medium, and large scenes. The top right image is the ground truth segmentation. The results from direct fusion [22], SSCNet [14], SemanticFusion [21] and ours are shown on the second row, respectively.

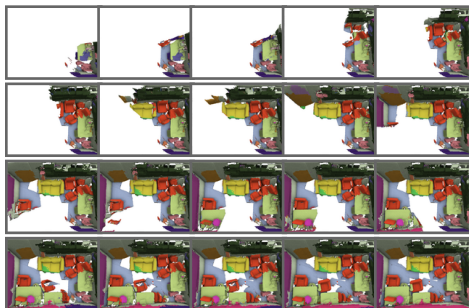
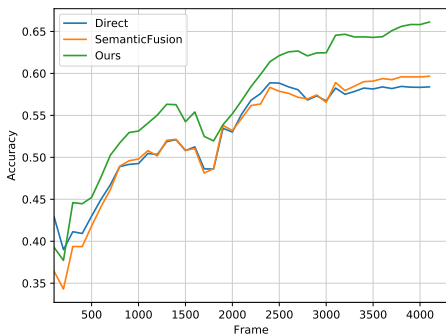
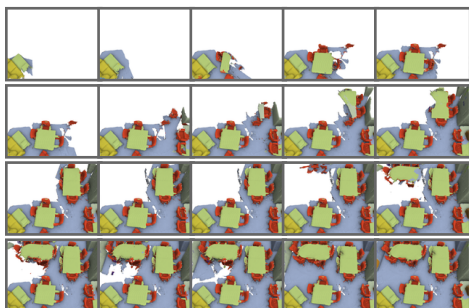
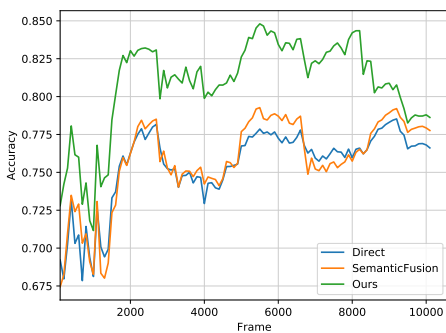
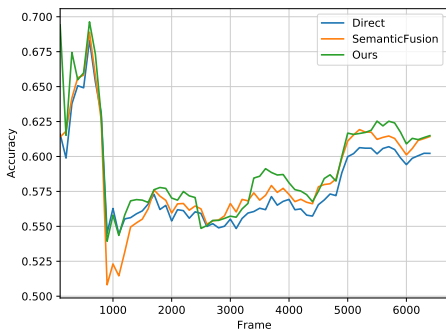
SceneNN/030*SceneNN/206**SceneNN/272*

Fig. 6: Temporal accuracy of different methods on selected scenes from SceneNN. The respective progressive semantic segmentation results of our method are shown on the right. Please refer to the supplementary materials for the full results.

References

1. Silberman, N., Hoiem, D., Kohli, P., Fergus, R.: Indoor segmentation and support inference from rgb-d images. In: ECCV. (2012) **1, 3, 10**
2. Gupta, S., Arbelaez, P., Malik, J.: Perceptual organization and recognition of indoor scenes from rgb-d images. In: Proceedings of the IEEE Conference on Computer Vision and Pattern Recognition. (2013) 564–571 **1**
3. Long, J., Shelhamer, E., Darrell, T.: Fully convolutional networks for semantic segmentation. In: CVPR. (2015) **1, 3, 10**
4. Hua, B.S., Pham, Q.H., Nguyen, D.T., Tran, M.K., Yu, L.F., Yeung, S.K.: Scenenn: A scene meshes dataset with annotations. In: International Conference on 3D Vision (3DV). (2016) **2, 9, 10, 12**
5. Dai, A., Chang, A.X., Savva, M., Halber, M., Funkhouser, T., Nießner, M.: Scannet: Richly-annotated 3d reconstructions of indoor scenes. In: Proc. Computer Vision and Pattern Recognition (CVPR), IEEE. (2017) **2, 9, 10**
6. Krähenbühl, P., Koltun, V.: Efficient inference in fully connected crfs with gaussian edge potentials. In: Advances in Neural Information Processing Systems (NIPS). (2011) **2, 8**
7. Chen, L.C., Papandreou, G., Kokkinos, I., Murphy, K., Yuille, A.L.: Semantic image segmentation with deep convolutional nets and fully connected crfs. arXiv preprint arXiv:1412.7062 (2014) **2**
8. Zheng, S., Jayasumana, S., Romera-Paredes, B., Vineet, V., Su, Z., Du, D., Huang, C., Torr, P.H.: Conditional random fields as recurrent neural networks. In: Proceedings of the IEEE International Conference on Computer Vision. (2015) 1529–1537 **2**
9. Arnab, A., Jayasumana, S., Zheng, S., Torr, P.H.: Higher order conditional random fields in deep neural networks. In: European Conference on Computer Vision, Springer (2016) 524–540 **2**
10. Yu, F., Koltun, V.: Multi-scale context aggregation by dilated convolutions. In: ICLR. (2016) **3**
11. Badrinarayanan, V., Kendall, A., Cipolla, R.: Segnet: A deep convolutional encoder-decoder architecture for image segmentation. arXiv preprint arXiv:1511.00561 (2015) **3, 8, 10**
12. He, K., Gkioxari, G., Dollár, P., Girshick, R.: Mask r-cnn. In: Computer Vision (ICCV), 2017 IEEE International Conference on, IEEE (2017) 2980–2988 **3**
13. Bai, M., Urtasun, R.: Deep watershed transform for instance segmentation. In: Computer Vision and Pattern Recognition (CVPR), 2017 IEEE Conference on, IEEE (2017) 2858–2866 **3**
14. Song, S., Yu, F., Zeng, A., Chang, A.X., Savva, M., Funkhouser, T.: Semantic scene completion from a single depth image. Proceedings of 30th IEEE Conference on Computer Vision and Pattern Recognition (2017) **3, 10, 13**
15. Qi, C.R., Su, H., Mo, K., Guibas, L.J.: Pointnet: Deep learning on point sets for 3d classification and segmentation. Proc. Computer Vision and Pattern Recognition (CVPR), IEEE (2017) **3**
16. Li, Y., Bu, R., Sun, M., Chen, B.: Pointcnn. arXiv:1801.07791 (2018) **3**
17. Hua, B.S., Tran, M.K., Yeung, S.K.: Pointwise convolutional neural networks. (2018) **3**
18. Newcombe, R.A., Izadi, S., Hilliges, O., Molyneaux, D., Kim, D., Davison, A.J., Kohli, P., Shotton, J., Hodges, S., Fitzgibbon, A.: Kinectfusion: Real-time dense surface mapping and tracking. In: The IEEE International Symposium on Mixed and Augmented Reality (ISMAR). (2011) **3, 4, 5**

19. Nießner, M., Zollhöfer, M., Izadi, S., Stamminger, M.: Real-time 3d reconstruction at scale using voxel hashing. *ACM Transactions on Graphics (TOG)* (2013) **3**, **4**, **5**
20. Valentin, J.P., Sengupta, S., Warrell, J., Shahrokni, A., Torr, P.H.: Mesh based semantic modelling for indoor and outdoor scenes. In: *CVPR*. (June 2013) **3**
21. McCormac, J., Handa, A., Davison, A., Leutenegger, S.: Semanticfusion: Dense 3d semantic mapping with convolutional neural networks. *arXiv preprint arXiv:1609.05130* (2016) **3**, **4**, **9**, **10**, **13**
22. Cavallari, T., Di Stefano, L.: Semanticfusion: Joint labeling, tracking and mapping. In: *Computer Vision–ECCV 2016 Workshops*, Springer (2016) 648–664 **4**, **9**, **13**
23. Papon, J., Abramov, A., Schoeler, M., Worgotter, F.: Voxel cloud connectivity segmentation-supervoxels for point clouds. In: *Proceedings of the IEEE Conference on Computer Vision and Pattern Recognition*. (2013) 2027–2034 **4**
24. Achanta, R., Shaji, A., Smith, K., Lucchi, A., Fua, P., Süsstrunk, S.: Slic superpixels compared to state-of-the-art superpixel methods. *IEEE transactions on pattern analysis and machine intelligence* **34**(11) (2012) 2274–2282 **4**
25. Karpathy, A., Miller, S., Fei-Fei, L.: Object discovery in 3d scenes via shape analysis. In: *Robotics and Automation (ICRA), 2013 IEEE International Conference on*, IEEE (2013) 2088–2095 **5**
26. Kanazaki, A., Harada, T.: 3d selective search for obtaining object candidates. In: *Intelligent Robots and Systems (IROS), 2015 IEEE/RSJ International Conference on*, IEEE (2015) 82–87 **5**
27. Felzenszwalb, P.F., Huttenlocher, D.P.: Efficient graph-based image segmentation. *International journal of computer vision* **59**(2) (2004) 167–181 **5**
28. Valentin, J., Vineet, V., Cheng, M.M., Kim, D., Shotton, J., Kohli, P., Nießner, M., Criminisi, A., Izadi, S., Torr, P.: Semanticpaint: Interactive 3d labeling and learning at your fingertips. *ACM Transactions on Graphics* (2015) **5**
29. Lin, T.Y., Maire, M., Belongie, S., Hays, J., Perona, P., Ramanan, D., Dollár, P., Zitnick, C.L.: Microsoft coco: Common objects in context. In: *European conference on computer vision*, Springer (2014) 740–755 **11**
30. Yu, L.F., Yeung, S.K., Tang, C.K., Terzopoulos, D., Chan, T.F., Osher, S.: Make it home: automatic optimization of furniture arrangement. *ACM Transactions on Graphics* **30**(4) (2011) 86 **13**